

1 **Influence of wood density in tree-ring based annual**  
2 **productivity assessments and its errors in Norway**  
3 **spruce.**

4

5

6 **O. Bouriaud<sup>1</sup>, M. Teodosiu<sup>2</sup>, A. V. Kirilyanov<sup>3,4</sup>, C. Wirth<sup>5,6</sup>**

7

8 [1] {National Research and Development Institute for Forestry, National Forest  
9 Inventory, Calea Bucovinei 73b, 725100 Câmpulung Moldovenesc, Romania}

10 [2] {National Research and Development Institute for Forestry, Calea Bucovinei 73b,  
11 725100 Câmpulung Moldovenesc, Romania}

12 [3] {V.N. Sukachev Institute of Forest SB RAS, Akademgorodok, Krasnoyarsk,  
13 660036 Russia}

14 [4] {Siberian Federal University, Krasnoyarsk, 660041, Russia}

15 [5] {Institute of Biology, University of Leipzig, Johannisallee 21-23, 04103 Leipzig,  
16 Germany}

17 [6] {German Centre for Integrative Biodiversity Research (iDiv) Halle-Jena-Leipzig,  
18 Deutscher Platz 5e, 04103 Leipzig, Germany}

19 Correspondence to: O. Bouriaud (obouriaud@gmail.com)

20

21 **Abstract**

22 Estimations of tree annual biomass increments are used by a variety of studies related  
23 to forest productivity or carbon fluxes. Biomass increment estimations can be easily  
24 obtained from diameter surveys or historical diameter reconstructions based on tree  
25 rings records. However, the biomass models rely on the assumption of a constant  
26 wood density. Converting volume increment into biomass also requires assumptions  
27 on the wood density. Wood density has been largely reported to vary both in time and  
28 between trees. In Norway spruce, wood density is known to increase with decreasing  
29 ring width. This could lead to underestimating the biomass or carbon deposition in  
30 bad years. The variations between trees of wood density has never been discussed but  
31 could also contribute to deviations. A modelling approach could attenuate these  
32 effects but will also generate errors.

33 Here were developed a model of wood density variations in Norway spruce, and an  
34 allometric model of volume growth. We accounted for variations in wood density  
35 both between years and between trees, based on specific measurements. We compared  
36 the effects of neglecting each variation source on the estimations of annual biomass  
37 increment. We also assessed the errors of the biomass increment predictions at tree  
38 level, and of the annual productivity at plot level.

39 Our results showed a partial compensation of the decrease in ring width in bad years  
40 by the increase in wood density. The underestimation of the biomass increment in  
41 those years reached 15%. The errors related to the use of an allometric model of  
42 volume growth were modest, around  $\pm 15\%$ . The errors related to variations in wood  
43 density were much larger, the biggest component being the inter-tree variability. The  
44 errors in plot-level annual biomass productivity reached up to 40%, with a full  
45 account of all the error sources.

46

47 Key words: Forest biomass, Uncertainty propagation, Bayesian framework, Wood  
48 density, Norway spruce, tree-ring

49

## 50 **1 Introduction**

51 Predicting trees biomass increment is a key step in quantifying and understanding  
52 forest productivity. Considerable efforts have been spent to evaluate forest  
53 productivity and carbon sink strength (Ciais et al., 2008). While productivity has long  
54 referred to volume growth, amply used in the forest management and displayed in  
55 yield tables, the focus recently switched to biomass, for its relationships with energy  
56 or carbon storage. Field-based estimations of biomass growth have a wide variety of  
57 applications, from forestry to carbon fluxes estimation, for example in comparison  
58 against eddy covariance (Barford et al., 2001; Rocha et al., 2006; Gough et al., 2008;  
59 Curtis et al., 2011; Ilvesniemi et al., 2011). Considerable efforts have been spent to  
60 estimate annual forest productivity in relation to climate fluctuations and forests  
61 carbon sink strength (Richardson et al., 2010; Wu et al., 2013). The importance of  
62 having both annual resolution and high spatial coverage has been illustrated by  
63 numerous studies (e.g. Reichstein et al., 2003; Ciais et al., 2005; Beer et al., 2010).  
64 Several methods are used to estimate forest productivity and carbon sink: eddy  
65 covariance, modelling, or field-based estimations such as inventories or tree-ring  
66 studies. Tree-ring based studies have the advantage of offering a large spatial  
67 covering, a potentially long time scale and also an annual resolution. They are  
68 therefore amply used to produce reference annual biomass production estimations, to  
69 compare against other methods (Beck et al., 2011; Babst et al., 2014a) or to bring  
70 complementary information (Babst et al., 2013). However several issues are  
71 associated to the use of tree-ring based estimations and the estimation of their error  
72 remains a critical poorly documented (Nickless et al., 2011).

73 In the reconstruction of the annual productivity or of the above-ground carbon uptake  
74 from field-based studies, one limiting element is the estimation of the wood density  
75 variations (Babst et al., 2014a). Indeed, volume increment time series can be produced  
76 by a variety of methods, such as the reconstruction of the diameter growth based on  
77 tree rings (Wirth et al., 2004; Rocha et al., 2006) or inventory reconstruction (Ohtsuka  
78 et al., 2007), but none of these methods bring information on the variation of wood  
79 density. Converting volume into biomass requires an estimation of the wood density,  
80 which is most likely based on literature and therefore neither related to site conditions,  
81 nor to trees growth rate, as for example in Vila et al., (2013). In the same manner,  
82 biomass equations implicitly rely on the use of an average and constant wood density

83 despite the many evidences of substantial wood density variations. In both cases,  
84 wood density is considered constant in time, and equal between trees.

85 Wood density has however been acknowledged as a highly variable characteristic and  
86 several major sources of annual density variations have been identified. Very high  
87 precision in the description of the wood density variations with new techniques (e.g.  
88 SilviScan, Evans, 1994) are possible but not widely available, while other techniques  
89 based on X-ray are rather time consuming and thus not applied to forest productivity  
90 studies. Within-tree variations occur at distinct time scales (Jyske et al., 2007). Over  
91 medium or long scales, annual wood density was proved to be related to ring age or to  
92 tree diameter, with higher values close to the pith in many species (Schweingruber,  
93 1988). At inter-annual scale, wood density variations can be substantial. There were  
94 several reports that (annual) ring density decreases with increasing ring width, for  
95 instance in Norway spruce (Bergqvist, 1998; Dutilleul et al., 1998; Lundgren, 2004;  
96 Bouriaud et al., 2005; Franceschini et al., 2010; 2013). Wood density was also proved  
97 to vary between trees (Wilhelmsson et al., 2002; Guilley et al., 2004), a fact which is  
98 never accounted for in studies using diameter surveys to produce biomass increment  
99 estimations.

100 The variations of wood density between trees and between years could compensate  
101 the variations in annual volume increment, or at least soften them. Recent studies  
102 brought evidences of such compensation, proving that neglecting annual wood density  
103 fluctuations could lead to substantial errors or bias in estimating the biomass (Molto  
104 et al., 2013; Babst et al., 2014a). The errors generated by neglecting the variations in  
105 wood density have been considered as small compared to those resulting from that of  
106 the volume increment estimation, but to our knowledge, such assumptions were never  
107 tested and the consequences not documented.

108 To be properly quantified, the consequences of neglecting wood density fluctuations  
109 between years and between trees had to be tested using an integrated approach,  
110 whereby the errors of the density model are propagated and combined with those of  
111 the model for volume growth. Such chain can be decomposed, and the impact of each  
112 step studied by modelling the steps into a single Monte Carlo Markov Chain (MCMC)  
113 process (e.g. Molto et al., 2013). Analytical solutions to estimate the biomass  
114 estimation error, based e.g. on Taylor expansion can sometimes be determined,  
115 depending on the model's complexity. But the errors of biomass increment, obtained

116 by subtracting subsequent estimations, are anyhow less predictable and particularly  
117 challenging at the plot level, when summing tree-level estimations (Nickless et al.,  
118 2011). The MCMC approach therefore appears as the most suitable to estimate the  
119 biomass increment, where such estimations and the propagation of the errors from one  
120 model to another is done without assumptions.

121 Our study aimed at quantifying the impact of density variations, both between years  
122 and between trees, on the estimations of annual biomass increment in Norway spruce  
123 (*Picea abies*), and compare it with the impact of volume increment estimation errors.  
124 The objectives were: (i) to quantify and model the influence of annual radial growth  
125 variations on wood density, (ii) to quantify the consequences of annual and between  
126 tree variations of wood density on biomass increment estimations and (iii) to compare  
127 the errors related to wood density estimations to those of volume increment.

128

129

## 130 **2 Material and methods**

131

### 132 **2.1 Site, sampling and data**

133 All samples analysed for this study were taken from the Wetzstein site near the village  
134 of Lehesten in Thuringia, Central Germany (50°45'N, 11°46'E, ~ 760 m a.s.l.), which  
135 was amply used for eddy covariance measurements (e.g. Anthoni et al., 2004) or  
136 biomass modeling (Wirth et al., 2004). The site is characterised by mono-specific  
137 Norway spruce (*Picea abies* L.) stands. The climate is typical for the mid-elevation  
138 montane sites with an annual mean temperature of 6°C and a mean annual  
139 precipitation sum of ~1000 mm. Soils have a sandy loam texture. The footprint of the  
140 eddy covariance tower is dominated by an extensive 80 ( $\pm 2.1$  SD) year old stand. This  
141 stand is mostly even-aged but also contains pockets of regeneration and scattered  
142 emergent trees. The footprint stand is surrounded by three even-aged stands with a  
143 mean age of 15 ( $\pm 0.86$ ), 38 ( $\pm 7.9$ ) and 116 ( $\pm 1.3$ ) years. The four stands representing  
144 the site are referred as W15, W38, W72 and W116

145 This study combines data from three successive samplings realized in this site: (i)  
146 Stem analysis performed to quantify the relationship between breast-height radial

147 growth and stem volume increment. This was achieved in connection with a biomass  
148 harvest of the four stands (see below). (ii) Wood density measurements were done for  
149 selected harvest trees to establish a relation between ring-width and wood density  
150 variations, and (iii) a dendro-chronological analysis of inter-annual growth variation  
151 of many trees using micro-cores for scaling up to the plot-scale. The volume  
152 increment and wood density and volume increment measurements are used  
153 exclusively to develop models, while the micro-cores sampling is used as an  
154 application to quantify and compare the errors of each model on this representative  
155 case study.

### 156 2.1.1 Stem analysis for volume increment

157 The stem volume increment model was fit based on a stem analysis realized on 22  
158 trees – seven samples in the footprint stand W72 and five in each of the additional  
159 stands (W15, W33, W116). Trees were selected to represent seven/five dbh (diameter  
160 at breast height) classes defined based on the population of all inventoried trees (W15:  
161  $n = 144$ , W38:  $n = 59$ , W72:  $n = 133$ , W116:  $n = 68$ ). Jointly, the 22 trees represented  
162 the size range (dbh between 7.3 and 59.5 cm) and age range (between 14 and 117  
163 years) of Norway spruce trees at the Wetzstein site. This comprehensiveness ensures  
164 applicability of the models for all trees in the inventories of the test site. Trees were  
165 felled in the context of a full biomass harvest. The circumference was measured every  
166 meter along the bole where a 3-8 cm thick disc was cut in order to determine annual  
167 increment along the entire stem. All discs were dried and sanded with a belt grinder.  
168 The ring width series was measured along four radii on each disc. The average  
169 diameter increment measured on the lower and upper disc of each 1 to 2 m segment  
170 was used to calculate the increment of under bark volume in successive years using  
171 the formula for a truncated cone. The difference in volumes of all segments per tree of  
172 successive annual time steps yielded stem dry wood production of individual trees.  
173 The dendrochronological analysis was carried out using a digital tree ring  
174 measurement device (LINTAB III Digital Linear Table; 410-1/100-HF-130, Frank  
175 Rinn Distribution, Heidelberg, Germany) in combination with the software TSAP  
176 (Time Series Analysis Program, Frank Rinn Distribution, Heidelberg, Germany).

177

### 178 2.1.2 Wood density measurements

179 For the annual wood density (WD) measurements wood discs were sampled at breast  
180 height from trees representing the lowest, the central and the highest diameter class in  
181 each of the four stands. This yielded a total of 12 sample trees, again representing the  
182 size and age range of Norway spruce tree at the site. Two 1-2 cm-wide slices from  
183 opposite radii were sawn from the wood discs, for which wood density was measured  
184 by X-ray densitometry in the densitometric Laboratory of Krasnoyarsk, Russia  
185 (Walesch Electronics, Switzerland) using the standard procedure described by  
186 Schweingruber (1988). Longitudinal strips with a constant thickness of 1.2 mm were  
187 sawn, air dried, and exposed to X-ray radiations for 1 h on a Kodak TL film using  
188 standard exposure conditions: acceleration tension of 8.5 kV, flux intensity of 15.0  
189 mA, distance to the source of 3.5 m. Annual wood density (WD,  $\text{kg m}^{-3}$ ) values were  
190 obtained from density profiles of single tree-rings as the total mass of earlywood and  
191 latewood divided by tree-ring width. X-ray derived densities represent dry wood.  
192 Rescaling to fresh wood dimensions was not done as all ring-width series (stem  
193 analysis and micro-cores) were measured on dry wood.

194

### 195 2.1.3 Application dataset

196 The volume increment and WD models were applied together on an independent set  
197 of trees sampled in 13 randomly placed inventory plots inside the footprint stand  
198 W72. The plots were established within the context of the project FORCAST (Rey  
199 and Jarvis, 2006). From 31 to 62 trees per plots (551 in total) with diameter varying  
200 from 8 to 51 cm (thus well within the range of the sample trees) were sampled for  
201 historical diameter reconstruction based on micro-cores. The micro-cores enabled the  
202 reconstruction of the past growth over the last 10 years only, since these short cores  
203 are ~2 cm long. The diameter was reconstructed based on the simple assumption of  
204 proportionality of the bark thickness to the diameter using the external diameter of the  
205 trees at sampling.

## 206 2.2 Wood density and annual volume increment modelling

207 Models of WD or annual volume increment were fit using both maximum likelihood  
208 methods and MCMC approach. The structure of the two models was first determined

209 using likelihood fits before being implemented in a Bayesian MCMC framework  
210 using WinBUGS 1.4 (Spiegelhalter et al., 2003), based on the same datasets exactly,  
211 using non-informative flat priors. The maximum-likelihood estimations were realized  
212 using the nlme package (version 3.1-102, Pinheiro et al., 2011) of R (R version 3.0.1,  
213 R Development Team, 2014).

214

### 215 2.2.1 The wood density model

216 Following recent publications on Norway spruce wood density (Franceschini et al.,  
217 2010; 2013), the diameter and the ring cambial age (as counted from the pith) were  
218 used as independent variables. The selection of the model was based both on the AIC  
219 (Akaike Information Criterion) and the examination of the residual distribution. Fixed  
220 and random tree-level effects were considered. The principle of parsimony was also  
221 followed in the model building process, and random effect parameters were  
222 considered only if improvements were observed based on the likelihood ratio test.

223 Several candidate models were tested, as follows

$$224 \quad WD_{ij} = a_0 + a_1RW_{ij} + a_2RW_{ij}^2 + \frac{a_3}{X_{ij}} + \varepsilon_{ij} \quad (1)$$

$$225 \quad WD_{ij} = a_0 + \frac{a_1}{1 + RW_{ij}} + \frac{a_2}{X_{ij}^{a_3}} + \varepsilon_{ij} \quad (2)$$

$$226 \quad WD_{ij} = a_0 + a_1RW_{ij}^{a_2} + \frac{a_3}{X_{ij}^{a_4}} + \varepsilon_{ij} \quad (3)$$

227 where  $i$  denotes the tree and  $j$  the year,  $a_0 \dots a_4$  are fixed effects and potentially random  
228 tree-level effects,  $X$  is either DBH or cambial age,  $\varepsilon \approx N(0, \sigma^2)$ . Random effects are  
229 assumed to be normally distributed.

230

### 231 2.2.2 The annual volume increment model

232 The annual volume increment was modelled as a non-linear function of ring width  
233 and tree diameter, based on the annual estimations of volume growth resulting from  
234 the detailed stem analysis. The model reflects the fact that, for a given ring width,  
235 volume increment depends strongly on the current size of the tree, here its diameter,

236 mostly for geometrical reasons. The taper was therefore not supposed to be constant  
237 in time, and the trends in tree growth with age were directly absorbed in the model  
238 since the volume increments resulted directly from the stem analysis measurements,  
239 not from using models. Another specificity of this model was the specification of a  
240 variance function in order to cope with the heteroscedasticity in the errors. The  
241 resulting model is given in equation 4 and includes random coefficients for the  
242 exponent  $b_3$ :

$$243 \quad \Delta Vol_{ij} = b_0 + b_1 DBH_{ij}^{b_2} RW_{ij}^{b_3} + \varepsilon_{ij} \quad (4)$$

244 where  $b_{3,i} = c_3 + d_{3,i}$  is the sum of a fixed parameter  $c_3$  and a random tree-level term  
245  $d_{3,i} \sim N(0, \sigma_{d3})$  that varied for each tree  $i$ .

246 The residual  $\varepsilon_{ij}$  was modeled as a power function of the diameter:

$$247 \quad \varepsilon_{ij} = b_4 + DBH^{b_5} \quad (5)$$

248

### 249 **2.3 Application to a case study, scenarios of biomass increment**

250 The micro-cores dataset was used as a concrete case study for estimating the  
251 consequences of wood density variations and comparing the errors resulting from the  
252 wood density and from the volume increment model. Both models were fit based on  
253 their specific datasets within the MCMC framework, then the parameters and the  
254 variance terms estimated were applied to compute the biomass increment of the  
255 micro-cores trees, which represents an external set. The models were therefore fit  
256 using the same structure as that used in the likelihood method, the parameters  
257 estimated being further used to produce estimations of WD or annual volume  
258 increment on the micro-core trees. Having both the fitting and the application run in a  
259 single MCMC loop enables the propagation of the errors of each model.

260 The tree-level biomass increment estimations were the product of the WD and the  
261 volume increment, then summed up to obtain stand-level per-ha biomass estimations  
262 based also on the plot size. But according to the way the errors could be accounted  
263 for, four different scenarios were distinguished:

264 1) The baseline scenario was using a constant wood density set to be equal to the  
 265 average observed value across the dataset ( $475 \text{ kg m}^{-3}$ ). The volume increment is  
 266 estimated based on the model fitted but without considering random tree-level  
 267 variations (using the fixed part of the model only) and without residual error ( $\varepsilon_{ij}=0$ ).

268 Thus, for tree  $i$  and year  $j$ , the biomass increment was computed as

$$269 \quad \Delta B_{ij} = 0.475 \cdot \Delta Vol_{ij} \quad \text{where } \Delta Vol_{ij} = b_0 + b_1 DBH_{ij}^{b_2} RW_{ij}^{b_3}$$

270 Only the fixed part of the parameters  $b_0$  to  $b_3$  was used.

271 2) In the second scenario, the annual wood density was held constant but the volume  
 272 increment included both the random tree-level variation and the residual error.

273 For tree  $i$  and year  $j$ , the biomass increment was computed as:

$$274 \quad \Delta B_{ij} = 0.475 \cdot \Delta Vol_{ij} \quad \text{with } \Delta Vol_{ij} = b_0 + b_1 DBH_{ij}^{b_2} RW_{ij}^{b_{3,i}} + \varepsilon_{ij} \quad (6)$$

275 where  $b_{3,i} = c_3 + d_{3,i}$  is the sum of a fixed parameter  $c_3$  and a random tree-level term  
 276 that varied for each tree  $i$  and sampled as:  $d_{3,i} \sim N(0, \sigma_{d_3})$ ,  $\sigma_{d_3}$  being estimated from  
 277 the volume increment fit dataset. Thus, the parameter  $d_3$  for the application varies  
 278 from tree to tree and is being sampled from within the variability observed in the fit  
 279 set.  $\varepsilon$  (the residual variation) is computed as a function of the diameter as presented  
 280 in Eq. 5. All the parameters and the variance estimations were made by the Bayesian  
 281 model within the MCMC loop.

282 3) In the third scenario, the biomass increment was defined as the product of the  
 283 parametric estimations of both the WD and the annual volume increment: here only  
 284 the fixed part of the models was used to produce both the WD and the volume  
 285 increment estimations, while not accounting for random effects or residual variance.  
 286 This represents the most common and probable use of such models, when no data are  
 287 available for a calibration.

$$288 \quad \Delta B_{ij} = WD_{ij} \cdot \Delta Vol_{ij} \quad \text{where}$$

$$289 \quad WD_{ij} = a_0 + a_1 RW_{ij}^{a_2} + \frac{a_2}{DBH_{ij}^{a_3}} \quad \text{and } \Delta Vol_{ij} = b_0 + b_1 DBH_{ij}^{b_2} RW_{ij}^{b_3}.$$

290 Only the fixed part of the parameters are used.

291 4) In the last scenario, a full error propagation was conducted: the random and the  
 292 residual errors of both the WD and the volume increment models were used to  
 293 produce the biomass increment estimation.

$$294 \quad \Delta B_{ij} = WD_{ij} \cdot \Delta Vol_{ij} \quad \text{with } WD_{ij} = a_{0,i} + a_{1,i} RW_{ij}^{a_2} + \frac{a_{3,i}}{DBH_{ij}^{a_4}} + \varepsilon_{ij}$$

295 having  $\forall k \in (0,1,3)$ ,  $a_{k,i} = \alpha_k + a_{k,i}$  where  $\alpha_k$  is the fixed part of the parameter,  $a_k$   
 296 the random component,  $a_{k,i} \sim N(0, \sigma_{ak})$  and  $\varepsilon_{ii} \sim N(0, \sigma_{WD})$  where  $\sigma_{WD}$  is the residual  
 297 variance, estimated on the WD fit set.

298  $\Delta Vol_{ij} = b_0 + b_1 DBH_{ij}^{b_2} RW_{ij}^{b_{3,i}} + \varepsilon_{ij}$  with  $b_{3,i} = c_3 + d_{3,i}$  and  $d_{3,i} \sim N(0, \sigma_{d3})$  as in scenario  
 299 2, and  $\varepsilon_{ii} \sim N(0, \sigma_{\Delta Vol})$  where  $\sigma_{\Delta Vol}$  is the residual variance, estimated on the  
 300 volume increment fit set.

301 Thus, four different biomass increment estimations were produced, according to the  
 302 density estimation and the error propagation, and their difference summed at plot  
 303 level. In all the scenarios, volume increment was estimated based on measured ring  
 304 width series and the historical diameter of the trees.

305 The MCMC process generated posterior distributions of the model parameter  
 306 estimates, with their associated errors, and the estimations of the variance of the  
 307 random effects based on the Metropolis-Hastings algorithm over  $10^4$  iterations. It also  
 308 produced estimations of wood density, a volume increment computed from the fitted  
 309 model and applied to new data, along with a prediction uncertainty interval, here  
 310 represented by the range between 2.5 and 97.5% of the estimates distribution density.  
 311 The first 4000 iterations were used as pre-convergence and thus were excluded from  
 312 estimations, which were based on subsequent iterations only.

313

### 314 **3 Results**

315

### 316 **3.1 Describing wood density variability**

317 The (annual) ring wood density (WD) varied from 287 to 787 kg m<sup>-3</sup> with within-trees  
318 variations as considerable as variations between trees. Individual tree-ring series  
319 showed a reduced WD in the first 5-10 years, followed by a linear increase up to 60  
320 years and then fluctuated around a tree-specific sill (Fig. 1a). Variations difference  
321 between two successive years reached 200 kg m<sup>-3</sup>.

322

323 Figure 1.

324

325 Variations in WD were mostly related to ring width with a linear correlation of -0.75  
326 ( $t = -39.23$ ,  $df = 1199$ ,  $p\text{-value} < 10^{-4}$ ) when pooling the data from all cores (Fig. 1b).  
327 As shown in figure 1, WD series with very distinct average density values were  
328 seemingly following the same linear pattern. The correlation with age was not as high  
329 ( $R_{\text{Pearson}} = 0.38$ ,  $t = 14.25$ ,  $df = 1199$ ,  $p\text{-value} < 10^{-4}$ ).

330

### 331 **3.2 Modelling annual wood density variability**

332 The selection of the WD model resulted from the comparison of several models based  
333 on independent variables such as ring width, cambial age and diameter. The models  
334 offered very comparable results (Table 1) although model 2 had a greater Root Mean  
335 Square Root (RMSE) and bias. Using cambial age or diameter as second independent  
336 variable did not lead to significant differences in the fit according to the Likelihood  
337 Ratio Test (LRT). Nevertheless, models differed in the ease of the convergence or on  
338 the sensitivity to initial parameters provided. The exponent parameters  $a_2$  and  $a_4$  of the  
339 independent variables (RW and X) being close to 0.5 in model 3, a simplification was  
340 tested which enabled to reduce the number of parameters and considerably eased the  
341 fitting, whereby both exponents were fixed to 0.5. This simplification did not lead to a  
342 significant change in the AIC. The model retained was therefore the model 4 derived  
343 from Eq. 3 with exponent parameters set to 0.5, and with the DBH as second  
344 independent variable, which is also a variable easier to measure than the cambial age.

345

346 Table 1.

347

### 348 **3.3 Modelling the annual volume increment**

349 The volume increment model was fit as a function of diameter and ring width, with  
350 fixed and random tree-level effects, to a set of 22 trees. The intercept was kept free  
351 after testing its significance using the LRT by comparing models with intercept held  
352 constant or forced to 0. It appeared that a free intercept increases the likelihood, while  
353 the estimated value of the intercept was very realistic. The use of a weight function  
354 (constant plus power) was also amply confirmed by the LRT (L.ratio=1368,  
355  $p<0.0001$ ). Thus, the final model consisted in a function of diameter and ring width,  
356 with fixed and random (tree level) parameters weighting (Table 2). The adequacy of  
357 the model was confirmed by the standardized residuals plot (Fig. 2).

358

359 Figure 2.

360 Table 2.

361

### 362 **3.4 The compensation problem: WD buffers annual volume increment** 363 **variations**

364 Provided that there was an overall decrease in wood density with increasing ring  
365 width, a compensation of ring width annual variability by wood density was also  
366 probable. The ring width series showed peak years of growth (e.g. 1967, 1989) or  
367 depressions (1976, 1983). In these years, the radial growth was much more affected  
368 than the wood density, as suggested by the deviations relative to the mean value  
369 calculated over the entire series length. The deviations peaked in 1967 at  $+30\pm 12\%$   
370 ( $\pm$ standard error), which means a radial growth greater than average by 30%, while  
371 the reduction of density was only  $-5\pm 2\%$ . In 1976, the growth reduction was  $-30\pm 6\%$   
372 but the density did not significantly increase:  $+1\pm 2\%$ . The consequences for biomass  
373 increment of neglecting the annual WD variations is further shown in Fig 3 where the  
374 biomass increment was estimated for the trees used for WD measurements. The  
375 annual volume increment was estimated by applying the model fitted (Eq. 4),

376 multiplied by either the annual WD values or by the mean WD for each tree and  
377 radius. The deviation between the two estimates are expressed as a percentage of the  
378 annual biomass increment using annual WD values. Although the deviations seemed  
379 random (Fig. 3a), their ordination in time proved that they were not, and that they  
380 exceeded 15% on average among all trees during extreme years (Fig. 3b).

381

382 Figure 3.

383

### 384 **3.5 Application to an independent data set**

385 The two models presented and fitted above were introduced in the Bayesian  
386 framework, with the same structure exactly and on the same data, and further re-fitted  
387 using the MCMC method. A comparison of the parameters estimated by both methods  
388 is presented in table 2. Expectedly, the parameters were not exactly the same but very  
389 close, and the correlation between the predictions was very high.

390 When applied on the independent application set, the estimated wood density varied  
391 from 278 to 541 kg m<sup>-3</sup>, with a mean of 425 (±35) kg m<sup>-3</sup> as a result of the variable  
392 ring-width and diameter input values. The model reproduced large between-tree  
393 differences for a given year, up to 225 kg m<sup>-3</sup>. Including random effects did not affect  
394 the prediction mean (Fig. 4). The overall (pooling trees from all plots together)  
395 average difference between the two predictions was only 0.1 kg m<sup>-3</sup>. The inclusion of  
396 the random effects changed the predictions only very marginally but increased the  
397 prediction interval five times: it jumped from ±20-40 kg m<sup>-3</sup> to ±160 kg m<sup>-3</sup>.  
398 Accounting for the residual variation (the epsilon term in Eq. 3) increased only  
399 slightly the prediction interval: it added an extra ±10 kg m<sup>-3</sup>.

400 Comparable results were obtained with the volume increment model: the contribution  
401 of the random effects and the inclusion of the residual variance inflated substantially  
402 the prediction interval (Fig. 4). Nevertheless, the relative prediction interval were  
403 substantially lower than that of the wood density: typically less than 40% of the  
404 predicted value, against 60% for WD.

405

406 Figure 4.

407

## 408 **3.6 Consequences of WD variations and error sources for the biomass** 409 **increment estimations**

### 410 3.6.1 At tree level

411 The annual variations of the predicted biomass increment resulting from considering a  
412 dynamic wood density were always smaller than predictions based on a constant  
413 density (Fig. 5). The prediction uncertainty was considerably higher when accounting  
414 for random effects on either the WD or the volume increment. The full error  
415 propagation (sc4) had a relative prediction uncertainty up to 60% of the predicted  
416 value on average, occasionally reaching or overcoming 100%. Constant density  
417 predictions had logically the lowest uncertainties (less than 10%) since they include  
418 only the error from the volume increment estimation. Wood density had the greatest  
419 contribution to the prediction uncertainty, and mainly through the between-tree  
420 variations. The parametric estimation (sc3) had a prediction interval four times lower  
421 than the full error propagation prediction (sc4), showing an underestimation of the  
422 error made by considering the uncertainty related to the regression coefficients only.

423

424 Figure 5.

425

### 426 3.6.2 At plot level

427 At plot level, which is the aggregation of the tree-level predictions and errors, the  
428 prediction errors tended to compensate each other since the relative prediction  
429 intervals of the annual biomass production were smaller than at tree-level (Fig. 6).  
430 Thus the interval of biomass production estimates varied from ~7% (sc1: no random  
431 effect, no residual error) to 10-30% (sc4: full error accounting) at stand level. It is  
432 noticeable that the relative prediction interval at 95% was never greater than 40%  
433 despite the combined errors of the two models (wood density and volume increment)  
434 plus the errors related to the random tree-level variations.

435

436 Figure 6.

437

438 The variation between years in the prediction error was also very low (Fig. 6) despite  
439 contrasted ring widths. The error of the predictions based on regression errors only  
440 (sc1 and sc3) did not vary with increasing number of trees in the plot (Fig. 6). In  
441 contrast, the predictions error decreased slightly with increasing number of trees for  
442 the scenarios that used a (tree-level) random-effect term (sc2 and sc4).

443

## 444 **4 Discussion**

### 445 **4.1 Overestimations of the variations in annual biomass increment under** 446 **constant density**

447 Wood density was found to decrease when ring width increased, in agreement with  
448 previous studies on Norway spruce (e.g. Olesen, 1976; Lindström, 1996; Dutilleul et  
449 al., 1998). Despite the seemingly high correlation between ring width and WD, the  
450 decrease of WD was not enough to compensate the increase in ring width but  
451 contributed to attenuate its effects. The order of magnitude of the WD variability was  
452 not -and by far- as large as that of ring width. Hence, it is logical to find a moderate  
453 compensation between radial growth and wood density variations even in extreme  
454 years such as 1976: 15% at plot level. Nevertheless, when the focus is put on key  
455 years, such as years of climatic extremes, the measurements of WD is necessary to  
456 avoid a systematic underestimation of the biomass increment or carbon uptake.  
457 Climate is indeed probably the most important driver of WD variations with  
458 influences at both inter- and intra-annual time steps (e.g. Gindl et al. 2000, Bouriaud  
459 et al. 2015). These results are consistent with those reported in Babst et al. (2014a)  
460 showing that accounting for the variations in WD strongly improved the match  
461 between the tree-ring based above-ground wood biomass increment estimations and  
462 the seasonal CO<sub>2</sub> fluxes measured by eddy covariance.

463 A constant value of wood density, such as implicitly used in a biomass equations, can  
464 generate systematic deviations because it has only few chances to be equal to the  
465 mean density of the trees to which the model is applied. Even if using a site-specific  
466 WD value, neglecting the radial increment of WD (i.e. the age-related trend) will also

467 lead to under-estimating the biomass increment. This source of error can  
468 unfortunately not be compensated by a larger sampling since it affects all the trees  
469 simultaneously. This has consequences not only for the annual productivity  
470 estimations but also for periodical productivity assessments, such as those conducted  
471 on permanent sample plots over a 5 or 10-years period.

472 Compensations of increased growth rate by a decrease in wood density was  
473 documented for Norway spruce but over a long time scale (Bontemps et al., 2013).  
474 The trends in radial growth and in WD reported for many species could lead to such  
475 deviations between the actual WD and the modelled or implicit WD. In this context, a  
476 local calibration would reduce such errors but cannot solve the problem of the  
477 variations between years and between trees.

478 The anticorrelation between ring width and wood density seems to be a general  
479 feature in Norway spruce according to the literature (e.g. Olesen, 1976; Lindström,  
480 1996; Dutilleul et al., 1998) but the phenomenon is not limited to this species (Babst  
481 et al., 2014). The attenuation therefore probably occurs at a large scale. The between-  
482 tree variability in the relationship has also been reported in several studies and  
483 probably is a widespread feature with potentially large consequences on the error of  
484 annual biomass increment predictions, as demonstrated by this study. The fact that the  
485 trees used to assess both the wood density variations and to model the volume  
486 increment came from the same site as those used for the error estimations has ruled  
487 out the issues of using locally inappropriate models. Additional errors should be  
488 considered in practice when using models that may not be locally valid.

## 489 **4.2 Predictions uncertainty**

490 The inventory-based or tree-ring-based estimations of annual biomass production or  
491 carbon uptake are often used for comparisons against other methods such as remote  
492 sensing, vegetation models or eddy covariance (Beck et al., 2011; Bunn et al. 2013;  
493 Babst et al., 2014a). To be conclusive, the benchmarking however supposes that  
494 prediction errors are known or can be estimated. High prediction errors would  
495 invalidate the biometric approaches but the errors are not always accounted for.  
496 Analytical solutions are indeed not always available to estimate the errors of the  
497 allometric models, and their estimation remains very complex or based on  
498 assumptions. In the case of the biomass increment, the error results from the

499 combination of several models, and the estimation is even more challenging. The use  
500 of the MCMC framework here avoids the cumbersome analytical approximations for  
501 prediction variances (e.g. Wutzler et al., 2008).

502 The prediction interval at plot level was on average between 20 and 40% of the  
503 predicted biomass increment value. The uncertainty related to the regression  
504 parameters were about 10% only for both models. Reduced variance may be inherent  
505 to the use of local trees and the Bayesian modelling (Zapata-Cuartas et al., 2012) but  
506 these values are similar to those found by Nickless et al. (2011) for biomass  
507 estimations following a parametric approach -as opposed to the MCMC method used  
508 here. Unlike our results, this study did however not include the random tree-level  
509 variations, which appeared to be quite an important source of uncertainty. Indeed,  
510 accounting for random tree-level variations in the relation between wood density and  
511 ring width increased the prediction interval of the tree-level biomass increment  
512 drastically (i.e. decreased the prediction confidence), by a factor of 5. Further errors  
513 related to the residual non-explained variance, were, in comparison, very small.  
514 Consequently, the prediction interval of the biomass annual increment at plot level  
515 increased twofold by accounting for the random-tree effects. Hence, the contribution  
516 of WD to the prediction error of the biomass increment was much larger than that of  
517 the volume increment model.

518 The tree-level prediction error (in percentage of the prediction value) was found to be  
519 greater than those at plot level. Thus, the compensations occurred at plot level when  
520 summing up trees predictions. We speculate that these compensations happen because  
521 the variations are centred by construction around zero and have both negative and  
522 positive values. This explains also why the mean prediction values were always  
523 unaffected by accounting for random effects. Hence, neglecting random effects  
524 affected more the prediction interval than the predictions themselves.

525

### 526 **4.3 Variations between trees**

527 The relation between wood density, ring width and cambial age were proven to  
528 fluctuate between trees sampled within a same stand for many species: oak (Guilley et  
529 al., 2004; Bergès et al., 2008), common beech (Bouriaud et al., 2004), Norway spruce  
530 (Mäkinen et al., 2002; Jaakola et al., 2005; Franceschini et al., 2010). For a given

531 radial growth rate, the trees are building more or less biomass and so storing more or  
532 less carbon, according to the density of the wood.

533 This fluctuation is considered random because it cannot be attributed to a measurable  
534 factor. Random tree-level variations were nevertheless reported as a major source of  
535 wood density variations in a population (Zhang et al., 1994; Guilley et al., 2004;  
536 Bouriaud et al., 2004; Jaakola et al., 2005). It is often hypothesized to be related to the  
537 genetics, although not proven. Provenience studies brought some insight on it (Hysten,  
538 1999; Rozenberg et al., 2004), but much of the determinism remains unknown. Other  
539 factors, such as crown development (Lindström, 1996), could also be invoked to  
540 explain this variation source in wood density.

541 The changes in silvicultural practices, whereby the focus is put on targeted  
542 individuals, further stress the importance of errors in tree-level estimations of biomass  
543 and biomass increments. The tree-level variations were the largest error source and  
544 showed that the inter-tree variations can be seen as a limitation to the tree-level  
545 biomass prediction. Despite the many evidences of tree-level random effects, this  
546 variation source was largely ignored. Our study proved that the between-tree  
547 variations in the relation between ring width and wood density -although within the  
548 same species- contributed the most to the uncertainty in the biomass increment  
549 predictions. The variations are hypothesized to follow a normal distribution  
550 (Lindström and Bates, 1990). Thus, at plot level, a compensation is likely to occur.  
551 But this situation may not be true for all samplings, and certain designs could generate  
552 additional biases in the biomass production estimations. In this study, all the trees in a  
553 plot were sampled. Other samplings, for instance the selection of the biggest trees in a  
554 plot as classically done in dendrochronology, could lead to serious deviations as it  
555 could involve sampling faster-growing trees. Apart from the bias in productivity  
556 caused by a sampling focusing on faster-growing trees (Nehrbass-Ahles et al., 2014),  
557 the productivity at stand level would probably generate an over-estimation related to a  
558 decreased wood density as trees producing larger rings would be sampled. Another  
559 issue in using the tree-ring parameters (width and density) to produce annual  
560 productivity estimations is the presence of autocorrelation or carry-over effects in the  
561 series, which are reflected in the derived productivity estimations but are generally  
562 not observed in the carbon fluxes measured or modeled (Babst et al. 2014a, b,  
563 Ramming et al. 2015).

#### 565 4.4 Modelling wood density for biomass increment

566 Apart from the climate, the two foremost used variables used to model annual WD  
567 variations are ring width and ring (cambial) age. The relation between WD and radial  
568 growth was strong in our study and probably dominant in Norway spruce but may not  
569 be so for other species. In beech, for example, the relation between ring width and  
570 WD was shown to be weak (Bouriaud et al., 2004) and there was no clear trend in  
571 WD related to the age neither. Several studies reported a lack of significant  
572 correlations between ring width and WD for Norway spruce (e.g. Dutilleul et al.,  
573 1998). The relative stability in annual WD values is not calling for a correction of the  
574 biomass increment in such situation. It is probable that variations in WD would affect  
575 the estimation of biomass increment in species for which a relationship with ring  
576 width was already observed such oaks (Zhang et al., 1993; Bergès et al., 2008) or  
577 larch (Karlman et al., 2005). The contribution to the error in the prediction of biomass  
578 production is however likely to be important.

579 Conversely to ring width, ring age was found to be only slightly influent on the annual  
580 wood density in Norway spruce. Ring age is often considered in density models for  
581 representing the age trend or for the variations observed near the pith –the juvenile  
582 versus mature wood transition (e.g. Franceschini et al., 2010). WD in Norway spruce  
583 has been shown to present an age-dependent trend from pith to bark (Dutilleul et al.,  
584 1998; Hylén, 1999; Mäkinen et al., 2002), apart from the juvenile wood effect. In our  
585 study, the juvenile effect was not included for simplicity (series were pruned to  
586 exclude the first 3 years) but also because rings near pith anyway are often missing  
587 when working with increment cores. Part of the age effect can be absorbed by the  
588 irregular ring width variations exhibited by trees growing in stands where thinnings  
589 induce successive episodes of growth surge.

590 Wood density should not be mistaken for stem specific gravity (Williamson et al.,  
591 2010). Bark has a different mass to volume ratio than wood. The contribution of bark  
592 to the annual increment is however negligible. The approximation made consist in  
593 stating that the variations in specific gravity are proportional to that of wood density.  
594 Variations in ring width and WD at upper stem positions were however documented  
595 for different species (Bouriaud et al., 2005; Repola, 2006; Van der Maaten-

596 Theunissen and Bouriaud, 2012). These variations were mostly in the sense of a lesser  
597 reduction in growth of upper stem parts during years of limited growth. Altogether  
598 with the WD density effect, these effects show that the reaction of trees to  
599 unfavourable climate conditions are exacerbated or over-estimated by the breast-  
600 height radial growth.

601

## 602 **5 Conclusion**

603 Annual variations in wood density were proved to compensate partially (up to 15%)  
604 the variations in radial growth. Ignoring the relation between ring width and wood  
605 density would result in an underestimation of the biomass production in bad years.  
606 The use of allometric equations generated estimations with large prediction intervals  
607 at tree level, up to 60%, but the prediction errors at plot level compensated each other.  
608 Most of the error in the prediction of a tree's annual biomass increment comes from  
609 the great between tree variability in wood density. Plot-level errors were found to  
610 range between 10 and 20% only. This study validates the approach based on historical  
611 diameter records for estimating tree annual biomass increment and stand annual  
612 biomass production, but a local calibration of the allometric models reduces  
613 considerably the prediction errors.

614

## 615 **6 Acknowledgements**

616 This work was supported by a grant of the Romanian National Authority for Scientific  
617 Research, CNCS-UEFISCDI, project number PN-II-ID-PCE-2011-3-0781. CW is  
618 thankful to Sebastian Weist and Ulrich Prusnitzki for help in the field and Anja Kahl  
619 for dendrochronological analysis. CW acknowledges the support of the Max-Planck  
620 Society. AVK acknowledges EU COST Action FP1106 STReESS. Ernst-Detlef  
621 Schulze and Reiner Zimmermann established the Wetzstein site.

622

623 **7 References**

- 624 Anthoni, P. M., Knohl, A., Rebmann, C., Freibauer, A., Mund, M., Ziegler, W., Kolle,  
625 O., and Schulze, E.D.: Forest and agricultural land use dependent CO<sub>2</sub> exchange in  
626 Thuringia, Germany. *Glob. Change Biol.*, 10(12), 2005-2019, 2004.
- 627 Babst, F., Poulter, B., Trouet, V., Tan, K., Neuwirth, B., Wilson, R., Carrer, M.,  
628 Grabner, M., Tegel, W., Levanic, T., Panayotov, M., Urbinati, M., Bouriaud, O.,  
629 Ciais, P., and Frank, D.: Site- and species-specific responses of forest growth to  
630 climate across the European continent. *Glob. Ecol. Biogeogr.*, 22(6), 706-717.  
631 doi: 10.1111/geb.12023, 2013.
- 632 Babst, F., Bouriaud, O., Papale, D., Gielen, B., Janssens, I.A., Nikinmaa, E., Ibrom,  
633 A., Wu, K., Bernhofer, C., Köstner, B., Grünwald, T., and Frank, D.: Above-ground  
634 woody carbon sequestration measured from tree rings is coherent with net ecosystem  
635 productivity at five eddy-covariance sites. *New Phytol.*, 201, 1289-1303.  
636 DOI: 10.1111/nph.12589, 2014a.
- 637 Babst, F., Alexander, M. R., Szejner, P., Bouriaud, O., Klesse, S., Roden, J., Ciais, P.,  
638 Poulter, B., Frank, D., Moore, J. P. and Trouet, V.: A tree-ring perspective on the  
639 terrestrial carbon cycle. *Oecologia*, 176(2), 307-322, 2014b.
- 640 Barford, C.C., Wofsy, S.C., Goulden, M.L., Munger, J.W., Pyle, E.H., Urbanski, S.  
641 P., Hutryra L., Saleska S.R., Fitzjarrald D., and Moore, K.: Factors controlling long-  
642 and short-term sequestration of atmospheric CO<sub>2</sub> in a mid-latitude forest. *Science*,  
643 294(5547), 1688-1691, 2001.
- 644 Beck, P.S.A., Juday, G.P., Alix, C., Barber, V.A., Winslow, S.E., Sousa, E.E., Heiser,  
645 P., Herriges, J.D., and Goetz, S.J.: Changes in forest productivity across Alaska  
646 consistent with biome shift. *Ecol. Lett.*, 14, 373–379, 2011.
- 647 Beer, C., Reichstein, M., Tomelleri, E., Ciais, P., Jung, M., Carvalhais, N.,  
648 Rödenbeck, C., Arain, M. A., Baldocchi, D., Bonan, G. B., Bondeau, A., Cescatti, A.,  
649 Lasslop, G., Lindroth, A., Lomas, M., Luysaert, S., Margolis, H., Oleson, K. W.,  
650 Rouspard, O., Veenendaal, E., Viovy, N., Williams, C., Woodward, F. I., and Papale,  
651 D.: Terrestrial gross carbon dioxide uptake: global distribution and covariation with  
652 climate, *Science*, 329, 834–838, 2010.

653 Bergès, L., Nepveu, G., and Franc, A.: Effects of ecological factors on radial growth  
654 and wood density components of sessile oak (*Quercus petraea* Liebl.) in Northern  
655 France. *Forest Ecol. Manage.*, 255(3), 567-579, 2008.

656 Bergqvist, G.: Wood density traits in Norway spruce understorey: effects of growth  
657 rate and birch shelterwood density. *Ann. Sci. For.*, 55(7), 809-821, 1998.

658 Bontemps, J.D., Gelhaye, P., Nepveu, G., and Hervé, J.C.: When tree rings behave  
659 like foam: moderate historical decrease in the mean ring density of common beech  
660 paralleling a strong historical growth increase. *Ann. Sci. For.*, 70(4), 1-15, 2013.

661 Bouriaud, O., Breda, N., Le Moguedec, G., and Nepveu, G.: Modelling variability of  
662 wood density in beech as affected by ring age, radial growth and climate. *Trees-*  
663 *Struct. Func.*, 18, 264-276, 2004.

664 Bouriaud, O., Leban, J.M., Bert, D., and Deleuze, C.: Intra-annual variations in  
665 climate influence growth and wood density of Norway spruce. *Tree Physiol.*, 25(6),  
666 651-660, 2005.

667 Bunn, A.G., Hughes, M.K., Kirilyanov, A.V., Losleben, M., Shishov, V.V., Berner,  
668 L.T., Oltchev, A., and Vaganov, E.A. 2013. Comparing forest measurements from  
669 tree rings and a space-based index of vegetation activity in Siberia. *Environ. Res.*  
670 *Lett.* 8, 035034, 2013. doi:10.1088/1748-9326/8/3/035034.

671 Ciais, P., Reichstein, M., Viovy, N., Granier, A., Oée, J., Allard, V., Aubinet, M.,  
672 Buchmann, N., Bernhofer, C., and Carrara, A.: Europe-wide reduction in primary  
673 productivity caused by the heat and drought in 2003: *Nature*, 437, 529–533, 2005.

674 Ciais, P., Schelhaas, M.J., Zaehle, S., Piao, S.L., Cescatti, A., Liski, J., Luysaert, S.,  
675 Le-Maire, G., Schulze, E.-D., Bouriaud, O., Freibauer, A., Valentini R., and Nabuurs,  
676 G.J.: Carbon accumulation in European forests. *Nat. Geoscience*, 1, 425–429,  
677 doi:10.1038/ngeo233, 2008.

678 Curtis, P., Hanson, P., Bolstad, P., Barford, C., Randolph, J., Schmid, H., and Wilson,  
679 K.: Biometric and eddy-covariance based estimates of annual carbon storage in five  
680 eastern North American deciduous forests. *Agr. Forest Meteorol.*, 113, 3-19, 2002.

681 Dutilleul, P., Herman, M., and Avella-Shaw, T.: Growth rate effects on correlations  
682 among ring width, wood density, and mean tracheid length in Norway spruce (*Picea*  
683 *abies*). *Can. J. Forest Res.*, 28(1), 56-68, 1998.

684 Evans, R.: Rapid Measurement of the Transverse Dimensions of Tracheids in Radial  
685 Wood Sections from *Pinus Radiata*. *Holzforschung*, 48(2), 168-172, 1994.

686 Franceschini, T., Bontemps, J.D., Gelhaye, P., Rittie, D., Herve, J.C., Gegout, J.C.,  
687 and Leban, J.M.: Decreasing trend and fluctuations in the mean ring density of  
688 Norway spruce through the twentieth century. *Ann. For. Sci.*, 67(8), 2010.

689 Franceschini, T., Longuetaud, F., Bontemps, J.D., Bouriaud, O., Caritey, B.D., and  
690 Leban, J.M.: Effect of ring width, cambial age, and climatic variables on the within-  
691 ring wood density profile of Norway spruce *Picea abies* (L.) Karst. *Trees-Struct.*  
692 *Func.*, 27(4), 913-925, 2013.

693 Gindl, W., Grabner, M., Wimmer, R.: The influence of temperature on latewood  
694 lignin content in treeline Norway spruce compared with maximum density and ring  
695 width. *Trees-Struct. Func.*, 14, 409-414, 2000.

696 Gough, C., Vogel, C., Schmid, H., and Curtis, P.: Controls on annual forest carbon  
697 storage: Lessons from the past and predictions for the future. *Bioscience*, 58: 609-622,  
698 2008.

699 Guilley, E., Hervé, J.C., and Nepveu, G.: The influence of site quality, silviculture  
700 and region on wood density mixed model in *Quercus petraea* Liebl. *Forest Ecol.*  
701 *Manage.*, 189(1), 111-121, 2004.

702 Hylen, G.: Age trends in genetic parameters of wood density in young Norway  
703 spruce. *Can. J. Forest Res.*, 29(1), 135-143, 1999.

704 Ikonen, V. P., Peltola, H., Wilhelmsson, L., Kilpeläinen, A., Väisänen, H., Nuutinen,  
705 T., and Kellomäki, S.: Modelling the distribution of wood properties along the stems  
706 of Scots pine (*Pinus sylvestris* L.) and Norway spruce (*Picea abies* (L.) Karst.) as  
707 affected by silvicultural management. *Forest Ecol. Manage.*, 256(6), 1356-1371,  
708 2008.

709 Ilvesniemi, H., Levula, J., Ojansuu, R., Kolari, P., Kulmala, L., Pumpanen, J.,  
710 Launiainen, S., Vesala, T., and Nikinmaa, E.: Long-term measurements of the carbon  
711 balance of a boreal Scots pine dominated forest ecosystem. *Boreal Environmental*  
712 *Research*, 14, 731-753, 2009.

713 Jaakkola, T., Mäkinen, H., and Saranpää, P. Wood density in Norway spruce: changes  
714 with thinning intensity and tree age. *Can. J. Forest Res.*, 35(7), 1767-1778, 2005.

715 Jyske, T., Makinen, H., and Saranpaa, P.: Wood density within Norway spruce stems.  
716 *Silva Fenn.*, 42(3), 439-455, 2008.

717 Karlman, L., Mörling, T., and Martinsson, O.: Wood density, annual ring width and  
718 latewood content in larch and Scots pine. *Eurasian J. Forest Res.*, 8(2), 91-96, 2005.

719 Lindström, H.: Basic density of Norway spruce. Part II. Predicted by stem taper, mean  
720 growth ring width, and factors related to crown development. *Wood Fiber Sci.*, 28(2),  
721 240-251, 1996.

722 Lindström, M.J., Bates, D.M.: Nonlinear mixed effects models for repeated measures  
723 data. *Biometrics*, 673-687, 1990.

724 Lundgren, C.: Microfibril angle and density patterns of fertilized and irrigated  
725 Norway spruce. *Silva Fenn.*, 38(1), 107-117, 2004.

726 Mäkinen, H., Saranpää, P., and Linder, S.: Wood-density variation of Norway spruce  
727 in relation to nutrient optimization and fibre dimensions. *Can. J. Forest Res.*, 32(2),  
728 185-194, 2002.

729 Molto, Q., Rossi, V., and Blanc, L.: Error propagation in biomass estimation in  
730 tropical forests. *Methods Ecol. Evol.*, 4, 175–183, doi:10.1111/j.2041-  
731 210x.2012.00266.x, 2012.

732 Nehrbass-Ahles, C., Babst, F., Klesse, S., Nötzli, M., Bouriaud, O., Neukom, R.,  
733 Dobbertin, M., and Frank, D.: The influence of sampling design on tree-ring based  
734 quantification of forest growth. *Glob. Change Biol.*, 20(9), 2867-2885, 2014.

735 Nickless, A., Scholes, R.J., and Archibald, S.: Calculating the variance and prediction  
736 intervals for estimates obtained from allometric relationships. *S. Afr. J. Sci.*  
737 2011;107(5/6), Art. #356, doi:10.4102/sajs.v107i5/6.356, 2011.

738 Ohtsuka T, Mo W, Satomura T, Inatomi M, and Koizumi H.: Biometric based carbon  
739 flux measurements and net ecosystem production (NEP) in a temperate deciduous  
740 broad-leaved forest beneath a flux tower. *Ecosystems*, 10, 324-334, 2007.

741 Pinheiro, J., Bates, D., DebRoy, S., and Sarkar, D.: R Development Core Team (2011)  
742 nlme: linear and nonlinear mixed effects models. R package version 3.1-98. R  
743 Foundation for Statistical Computing, Vienna, 2011.

744 Ramming, A., Wiedermann, M., Donges, J.F., Babst, F., von Bloh, W., Frank, D.,  
745 Thonicke, K. and Mahecha, M.D.: Coincidences of climate extremes and anomalous  
746 vegetation responses: comparing tree ring patterns to simulated productivity.  
747 *Biogeosciences*, 12, 373-385, 2015.

748 Repola, J.: Models for vertical wood density of Scots pine, Norway spruce and birch  
749 stems, and their application to determine average wood density. *Silva Fenn.*, 40(4),  
750 673-685, 2006.

751 Rey, A.N.A., and Jarvis, P.: Modelling the effect of temperature on carbon  
752 mineralization rates across a network of European forest sites (FORCAST). *Glob.*  
753 *Change Biol.*, 12(10), 1894-1908, 2006.

754 Reichstein, M., Ciais, P., Papale, D., Valentini, R., Running, S., Viovy, N., Cramer,  
755 W., Granier, A., Ogee, J., Allard, V., Aubinet, M., Bernhofer, C., Buchmann, N.,  
756 Carrara, A., Grünwald, T., Heimann, M., Heinesch, B., Knohl, A., Kutsch, W.,  
757 Loustau, D., Manca, G., Matteucci, G., Miglietta, F., Ourcival, J. M., Pilegaard, K.,  
758 Pumpanen, J., Rambal, S., Schaphoff, S., Seufert, G., Soussana, J. F., Sanz, M. J.,  
759 Rey, A.N.A., and Jarvis, P.: Modelling the effect of temperature on carbon  
760 mineralization rates across a network of European forest sites (FORCAST). *Glob.*  
761 *Change Biol.*, 12(10), 1894-1908, 2006.

762 Richardson, A. D., Black, T. A., Ciais, P., Delbart, N., Friedl, M. A., Gobron, N.,  
763 Hollinger, D. Y., Kutsch, W. L., Longdoz, B., and Luysaert, S.: Influence of spring  
764 and autumn phenological transitions on forest ecosystem productivity, *Philos. T. R.*  
765 *Soc. B*, 365, 3227–3246, 2010.

766 Rocha A, Goulden M, Dunn A, and Wofsy S.: On linking interannual tree ring  
767 variability with observations of whole-forest CO<sub>2</sub> flux. *Glob. Change Biol.*, 12, 1378-  
768 1389, 2006.

769 Rozenberg, P., Schüte, G., Ivkovich, M., Bastien, C., and Bastien, J.C.: Clonal  
770 variation of indirect cambium reaction to within-growing season temperature changes  
771 in Douglas-fir. *Forestry*, 77, 257–268, 2004.

772 Spiegelhalter, D.J., Thomas, A., Best, N., and Lunn, D.: WinBugs 1.4 [computer  
773 program]. Cambridge, UK: MRC Biostatistics Unit, Cambridge University, 2003.

774 Schweingruber, F.H.: *Tree rings and environment: dendroecology*. Paul Haupt AG  
775 Bern, 1996.

776 van der Maaten-Theunissen, M., and Bouriaud, O.: Climate–growth relationships at  
777 different stem heights in silver fir and Norway spruce. *Can. J. Forest Res.*, 42(5), 958-  
778 969, 2012.

779 Vesala, T., and Zhao, M.: Reduction of ecosystem productivity and respiration during  
780 the European summer 2003 climate anomaly: a joint flux tower, remote sensing and  
781 modelling analysis, *Glob. Change Biol.*, 13, 634–651, 2007.

782 Vilà, M., Carrillo-Gavilán A., Vayreda J., Bugmann H., Fridman J., Grodzki W.,  
783 Haase J., Kunstler G., Schelhaas M.J., and Trasobares A.. "Disentangling Biodiversity  
784 and Climatic Determinants of Wood Production." *PloS One*, 8(2), e53530, 2013.

785 Wilhelmsson, L., Arlinger, J., Spångberg, K., Lundqvist, S.O., Grahn, T., Hedenberg,  
786 Ö., and Olsson, L.: Models for predicting wood properties in stems of *Picea abies* and  
787 *Pinus sylvestris* in Sweden. *Scand. J. Forest Res.*, 17(4), 330-350, 2002.

788 Williamson, G.B., and Wiemann, M.C.: Measuring wood specific gravity... correctly.  
789 *Am. J. Bot.*, 97(3), 519-524, 2010.

790 Wimmer, R., and Downes, G.M.: Temporal variation of the ring width-wood density  
791 relationship in Norway spruce grown under two levels of anthropogenic disturbance.  
792 *IAWA*, 24(1): 53-61, 2003.

793 Wirth, C., Schumacher, J., and Schulze, E.D.: Generic biomass functions for Norway  
794 spruce in Central Europe—a meta-analysis approach toward prediction and  
795 uncertainty estimation. *Tree Physiol.*, 24(2), 121-139, 2004.

796 Wu, X., Mahecha, M.D., Reichstein, M., Ciais, P., Wattenbach, M., Babst, F., Frank,  
797 D., and Zang, C.: Climate-mediated spatiotemporal variability in the terrestrial  
798 productivity across Europe. *Biogeosciences Discuss.*, 10, 17511–17547, 2013.

799 Wutzler, T., Wirth, C., and Schumacher, J.: Generic biomass functions for Common  
800 beech (*Fagus sylvatica*) in Central Europe: predictions and components of  
801 uncertainty. *Can. J. Forest Res.*, 38(6), 1661-1675, 2008.

802 Zapata-Cuartas, M., Sierra, C.A., and Alleman, L.: Probability distribution of  
803 allometric coefficients and Bayesian estimation of aboveground tree biomass. *Forest*  
804 *Ecol. Manage.*, 277, 173-179, 2012.

805 Zhang, S.Y., Owoundi, R.E., Nepveu, G., Mothe, F., and Dhôte, J.F.: Modelling wood  
806 density in European oak (*Quercus petraea* and *Quercus robur*) and simulating the  
807 silvicultural influence. *Can. J. Forest Res.*, 23(12), 2587-2593, 1993.

808 Zhang, S.Y., Nepveu, G., and Owoundi, R.E.: Intratree and intertree variation in  
809 selected wood quality characteristics of European oak (*Quercus petraea* and *Quercus*  
810 *robur*). *Can. J. Forest Res.*, 24(9), 1818-1823, 1994.

811

812 **Tables and figure captions**

813 Table 1. Fit statistics and parameters for the wood density models.

814 Table 2. Comparison of the fixed parameters estimated for the wood density and the  
815 volume models, obtained by maximum likelihood and MCMC. Standard deviations  
816 are provided in brackets.

817

818 Figure 1. Relation between annual wood density and cambial age (left) or ring width  
819 (right) at tree level. Two trees with very distinct average wood density were  
820 highlighted (dark gray/black colors).

821

822 Figure 2. Observed and fitted annual volume increment model and standardized  
823 residuals of the volume increment model fit.

824

825 Figure 3. Left, Comparison of biomass increment estimations for Norway spruce trees  
826 growing in Wetzstein, based on constant density hypothesis vs actual wood density  
827 measurements; Right, time-course of the average ratio of biomass increment  
828 estimations (actual over constant density) and time-course of the detrended mean ring  
829 width (spline smoothing, for illustration purposes).

830 The  $\pm 2sd$  interval for the average biomass ratio is displayed as a gray band.

831

832 Figure 4. Left, variations of the MCMC annual predictions and prediction intervals  
833 (95%) of wood density and volume increment for one given tree randomly chosen  
834 while accounting for different error sources: regression only/regression and random  
835 effects/regression, random effects and residual variance; Right, distribution density of  
836 the relative prediction interval (expressed in percentage of the prediction) for all trees  
837 used for the simulation, according to the error sources included.

838

839 Figure 5. Annual biomass increment (posterior MCMC distribution) for one given tree  
840 chosen as representative with its associated prediction error for scenario 1 and 2 (a) or

841 scenario 3 and 4 (b); c) distribution density of relative prediction interval (expressed  
842 in percent of the prediction) for all trees used for the simulation, according to the  
843 scenario. Scenario 1 is based on constant WD and no random or residual error from  
844 the volume increment model, Scenario 2 is based on constant WD and random error  
845 in the volume increment model, Scenario 3 is based on modelled WD but without  
846 random and residual error accounting, Scenario 4 is based on modelled WD and  
847 volume increment with a full error accounting (see section 2.3 for more details).

848

849 Figure 6. Plot-level annual relative prediction intervals of the biomass increment as a  
850 function of the number of trees sampled in the plot for the 4 scenarios (a). Distribution  
851 density of the relative prediction interval of the biomass increment at plot level, all  
852 plots pooled, (b).

853

854

855

Table 1

856

Eq.	Model	Fixed effect	df	AIC	RMSE	Bias
					kg m <sup>-3</sup>	kg m <sup>-3</sup>
1	WD = $a_0 + a_1 \cdot RW + a_2 \cdot RW^2 + a_3 / X^{0.5}$	RW, CBA	12	12549	44.62	0.135
		RW, DBH	12	12567	44.90	0.135
2	WD = $a_0 + a_1 / (1 + RW) + a_2 / X^{0.5}$	RW, CBA	11	12770	60.24	0.874
		RW, DBH	11	12802	64.70	0.674
3	WD = $a_0 + a_1 \cdot RW^{a_2} + a_3 / X^{a_4}$	RW, CBA	12	12554	44.90	0.018
		RW, DBH	12	12569	45.15	-0.046
4	WD = $a_0 + a_1 RW^{0.5} + a_2 / X^{0.5}$	RW, CBA	11	12552	44.92	-0.019
		RW, DBH	11	12567	45.20	-0.073

857

858

859

860

861

862

863

WD: (annual) wood density, RW: (annual) ring width, X: either cambial age (CBA) or diameter (DBH).

Models 1 to 3 correspond to equations 1-3 presented in the section 2.2.1, and model 4 corresponds to equation 3 with parameter  $a_2$  and  $a_4$  set to 0.5.

They were 1201 observations, 10 groups.

864

Table 2

865

Model	Parameters	Likelihood fit	MCMC fit
$WD = a_0 + a_1 RW^{0.5} + a_2 / DBH^{0.5} + e$	$a_0$	594.33 (16.11)	555.10 (20.04)
	$a_1$	-10.09 (0.43)	-9.23 (0.70)
	$a_2$	13.93 (41.21)	17.13 (29.00)
	$e$	2054	2083 (93)
$\Delta V = b_0 + b_1 DBH^{b_2} RW^{b_3} + e$	$b_0$	0.284 (0.041)	0.047 (0.005)
	$b_1$	0.161 (0.012)	0.009 (0.001)
	$b_2$	1.820 (0.034)	1.733 (0.011)
	$b_3$	0.645 (0.019)	0.649 (0.019)
	$e = b_4 + DBH^{b_5}$	9.316e-03	0.283 (0.136)
	$b_4$	15.505	-0.093 (0.009)
	$b_5$	1.871	0.225 (0.005)

866

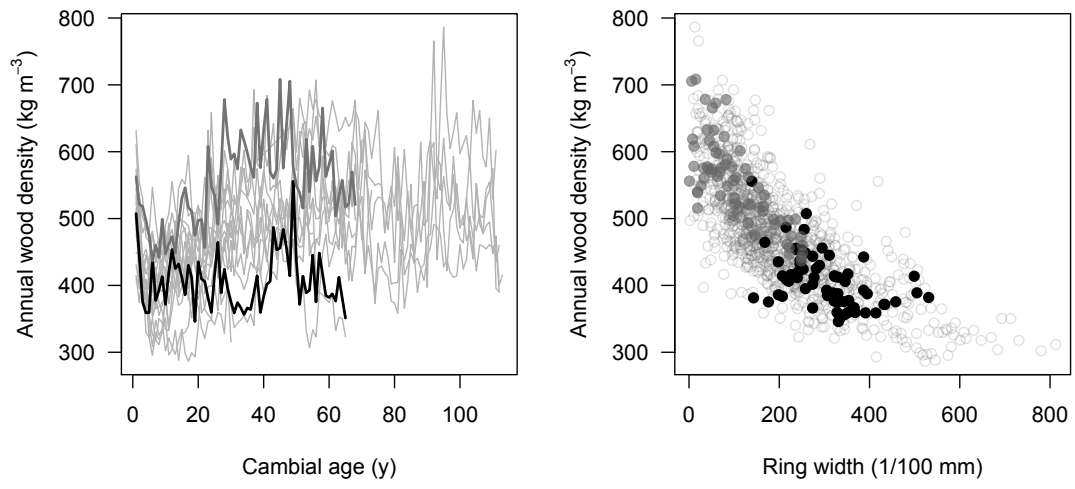
867

WD: (annual) wood density, RW: (annual) ring width, DBH: (annual) breast-height diameter, e: residual error.

868

869

Figure 1

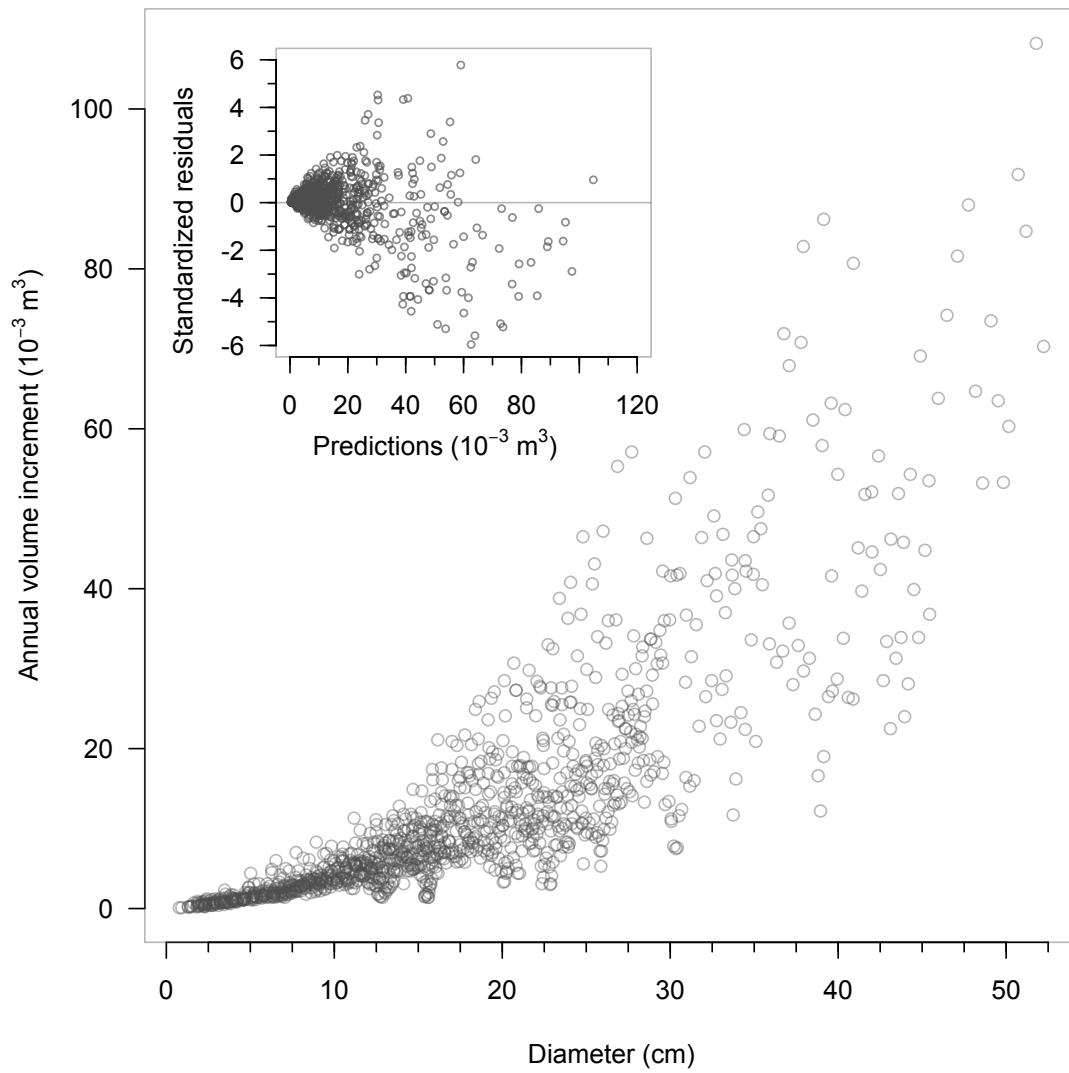


870

871

872

Figure 2



873

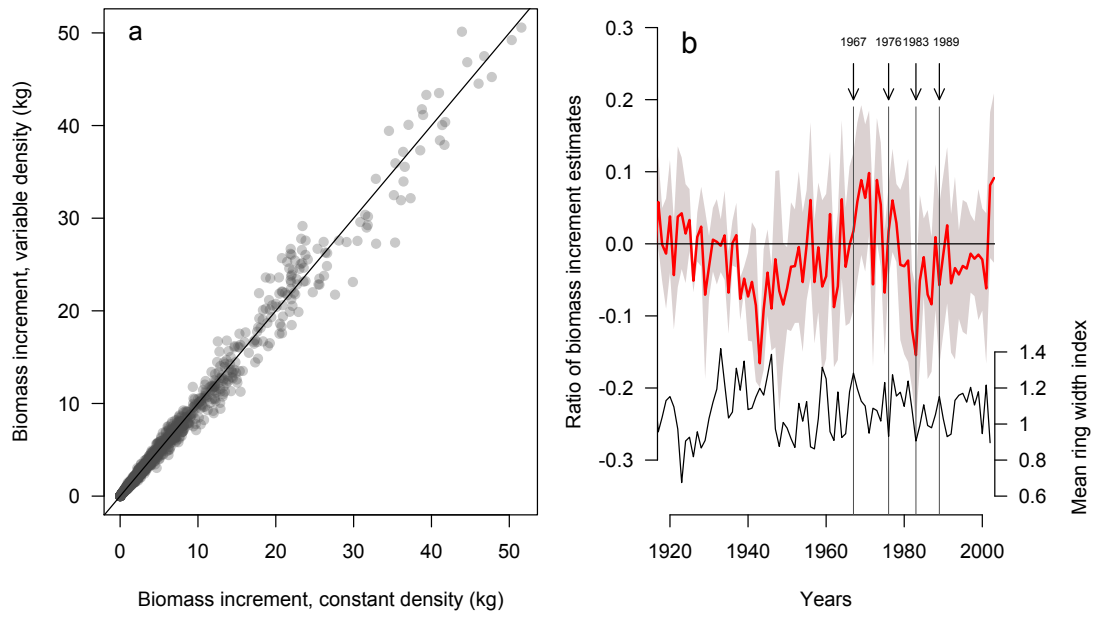
874

875

876

Figure 3

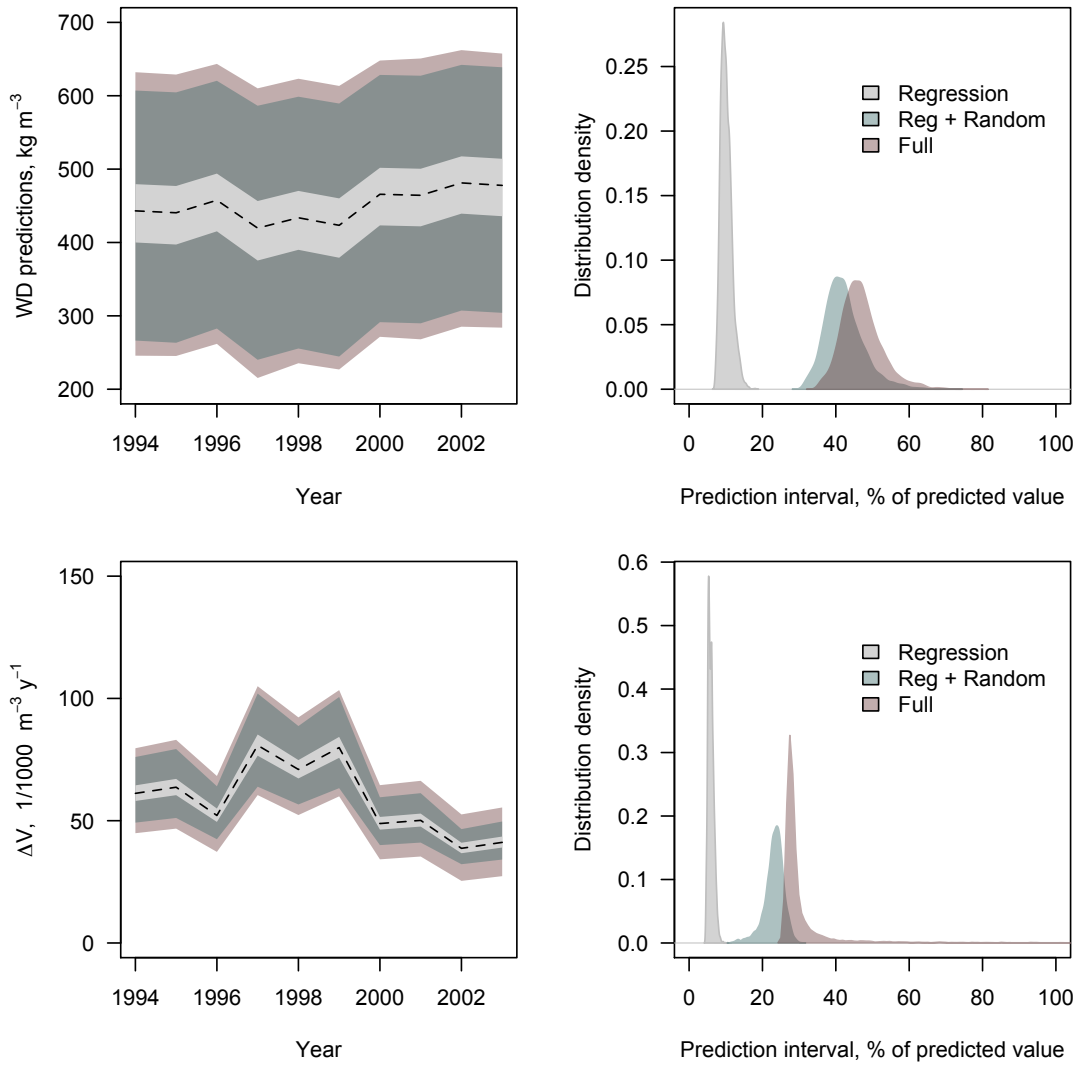
877



878

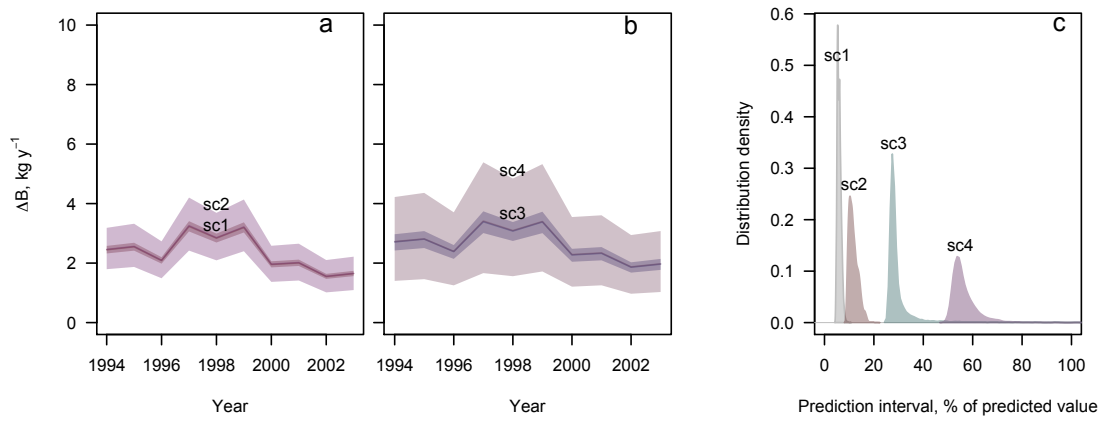
879

Figure 4



883

Figure 5

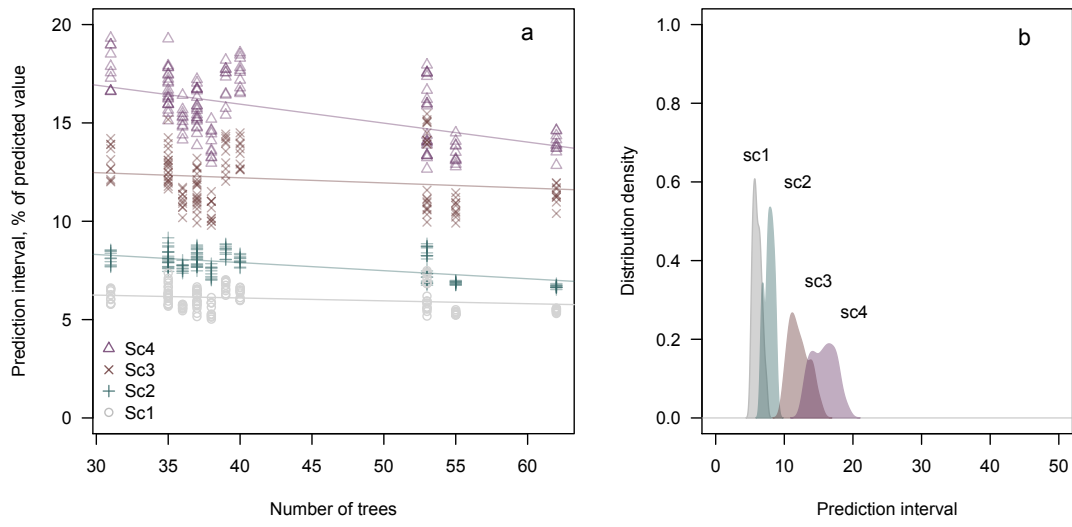


884

885

886

Figure 6



887